Propagation Properties of Striplines Periodically Loaded with Crossing Strips

JEAN-FU KIANG, SAMI M. ALI, SENIOR MEMBER, IEEE, AND JIN AU KONG, FELLOW, IEEE

Abstract — **A rigorous dyadic Green's function formulation in the spectral domain is used to study the dispersion characteristics of signal striplines in the presence of metallic crossing strips.**

A set of coupled vector integral equations for the current distribution on the conductors is derived. Galerkin's method is then applied to derive the matrix eigenvalue equation for the propagation constant. The dispersion properties of the signal lines are studied for the two cases of finite and infinite length crossing strips.

The effects of the structure dimensions on the passband and stopband characteristics are investigated. For crossing strips of finite length, the stopband is mainly affected by the period, the crossing strip length, and the separation between the signal and the crossing strips. For crossing strips of infinite length carrying traveling waves, attenuation along the signal line exists over the whole frequency range of operation.

I. Introduction

IN MICROELECTRONIC computer packaging, a problem of practical interest is the study of propagation characteristics of microstrip lines embedded in a layered medium in the presence of periodic crossing metallic strips.

The analysis of striplines and finlines with periodic stubs has been studied by Kitazawa and Mittra [1], where a technique based on the network-analytical formulation is used. A slow-wave coplanar waveguide on periodically doped semiconductor substrate has been carried out by Fukuoka and Itoh [2]. Gu and Kong [3] used a quasi-static approach to study single and coupled lines with capacitively loaded junctions. The propagation characteristics of signal lines in a mesh-plane environment has been presented by Rubin [4]. More recently, the propagation characteristics of signal lines in the presence of periodically perforated ground plane was studied by Chan and Mittra [5].

An analysis of a width-modulated microstrip periodic structure using a quasi-static approach is presented in [6]. A hybrid spectral-domain analysis for similar periodic structures has been carried out in [7].

In this paper, a hybrid-mode analysis is used to study the propagation characteristics of striplines periodically loaded with crossing metallic strips. The periodic crossing strips are assumed to have finite or infinite length. A dyadic Green's function formulation for the periodically loaded structure is derived. A coupled set of vector integral equations for the surface current distribution is formulated. Galerkin's method is then applied to transform the resulting set of integral equations for the current distribution into a determinantal equation from which the dispersion characteristics are obtained.

The propagation properties of one signal line and two coupled lines in the presence of periodic crossing strips are investigated. Numerical results for the passband and stopband characteristics are presented.

Manuscript received June 22, 1988; revised October 28, 1988. This work was supported by the RADC under Contract F19628-88-K-0013, by the ARO under Contract DAAL03-88-J-0057, by the Joint Services Electronics Program under Contract DAAL03-86-K-0002, by the ONR under Contract N00014-86-K-0533, and by the NSF under Grant 8620029-ECS.

The authors are with the Department of Electrical Engineering and Computer Science, Massachusetts Institute of Technology, Cambridge, MA 02139.

IEEE Log Number 8826035.

II. Dyadic Green's Function Formulation

The geometrical configuration of the problem is shown in Fig. 1, where M signal striplines located at $z = z_m$, $m = 1, 2, \cdots, M$, are periodically loaded with crossing metallic strips having a period p. The crossing strips are of width w_c and length L_c, and are located in the plane $z = z_{M+1}$. Both the signal lines and the crossing strips are embedded in the same layer (l) having parameters (ϵ_l, μ_0).

In general, the electric field can be expressed in terms of the dyadic Green's function and the current distribution on the strip surfaces as [8]

$$\boldsymbol{E}_l(\bar{\boldsymbol{r}}) = i\omega\mu_l \iiint_V \bar{\bar{G}}_{ll}(\boldsymbol{r}, \boldsymbol{r}') \cdot \boldsymbol{J}(\boldsymbol{r}')\, dV' \tag{1}$$

where $\bar{\bar{G}}_{ll}(\bar{\boldsymbol{r}}, \boldsymbol{r}')$ is the dyadic Green's function when both the observation point $\boldsymbol{r}$ and the source point $\boldsymbol{r}'$ are located in the lth layer of the stratified medium. For $z > z'$,

$$\begin{aligned}\bar{\bar{G}}_{ll}(\boldsymbol{r}, \boldsymbol{r}') &= \frac{i}{8\pi^2} \iint_{-\infty}^{\infty} d\boldsymbol{k}_s e^{i\boldsymbol{k}_s \cdot (\boldsymbol{r}_s - \boldsymbol{r}_s')} \frac{1}{k_{lz}} \left\{ \frac{1}{\left(1 - R_{\cup l}^{\mathrm{TE}} R_{\cap l}^{\mathrm{TE}} e^{2ik_{lz}h_l}\right)} \right. \\ &\quad \left[\hat{h}(k_{lz}) e^{ik_{lz}z_l} + R_{\cup l}^{\mathrm{TE}} \hat{h}(-k_{lz}) e^{ik_{lz}(2h_l - z_l)}\right] \\ &\quad \left[\hat{h}(k_{lz}) e^{-ik_{lz}z_l'} + R_{\cap l}^{\mathrm{TE}} \hat{h}(-k_{lz}) e^{ik_{lz}z_l'}\right] \\ &\quad + \frac{1}{\left(1 - R_{\cup l}^{\mathrm{TM}} R_{\cap l}^{\mathrm{TM}} e^{2ik_{lz}h_l}\right)} \\ &\quad \left[\hat{v}(k_{lz}) e^{ik_{lz}z_l} + R_{\cup l}^{\mathrm{TM}} \hat{v}(-k_{lz}) e^{ik_{lz}(2h_l - z_l)}\right] \\ &\quad \left. \left[\hat{v}(k_{lz}) e^{-ik_{lz}z_l'} + R_{\cap l}^{\mathrm{TM}} \hat{v}(-k_{lz}) e^{ik_{lz}z_l'}\right] \right\}. \end{aligned} \tag{2a}$$

0018-9480/89/0400-0776$01.00 ©1989 IEEE

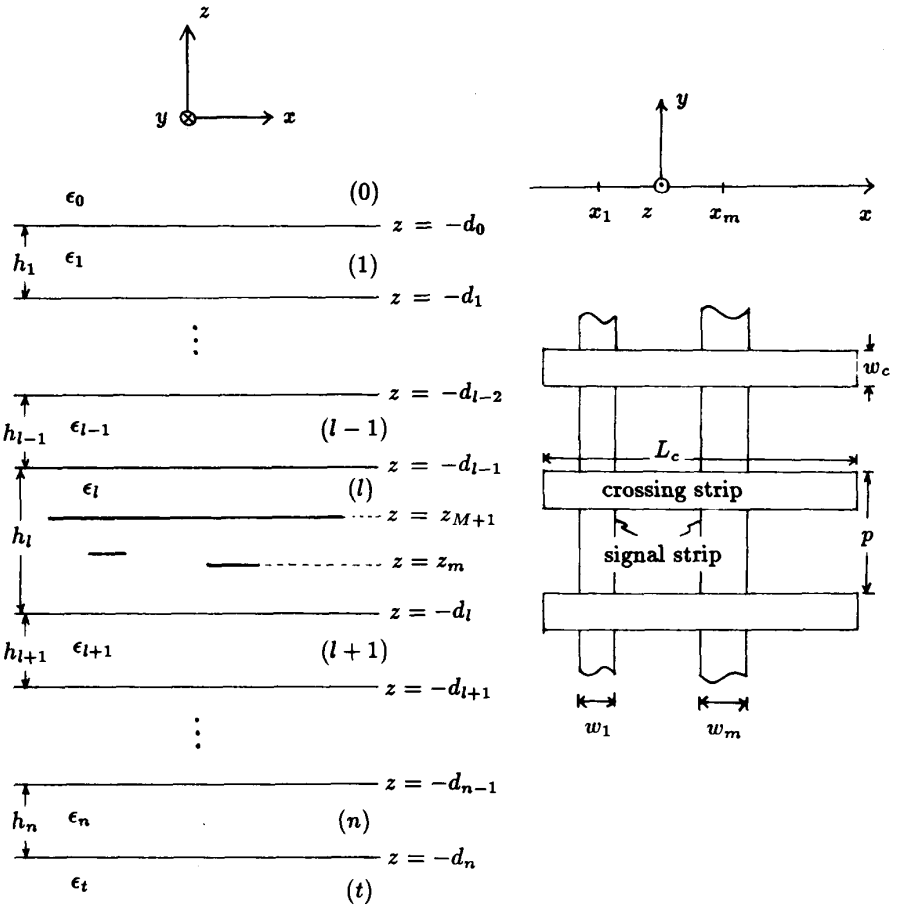

Fig. 1. Geometrical configuration of signal striplines periodically loaded with crossing metallic strips embedded in layer (l) of a stratified medium.

For $z < z'$,

$$\bar{\bar{G}}_{ll}(\boldsymbol{r}, \boldsymbol{r}')$$

$$= \frac{i}{8\pi^2} \iint_{-\infty}^{\infty} d\boldsymbol{k}_s e^{i\boldsymbol{k}_s \cdot (\boldsymbol{r}_s - \boldsymbol{r}_s')} \frac{1}{k_{lz}} \left\{ \frac{1}{\left(1 - R_{\cup l}^{\mathrm{TE}} R_{\cap l}^{\mathrm{TE}} e^{2ik_{lz}h_l}\right)} \right.$$

$$\left[\hat{h}(-k_{lz}) e^{-ik_{lz}z_l} + R_{\cap l}^{\mathrm{TE}} \hat{h}(k_{lz}) e^{ik_{lz}z_l}\right]$$

$$\left[\hat{h}(-k_{lz}) e^{ik_{lz}z_l'} + R_{\cup l}^{\mathrm{TE}} \hat{h}(k_{lz}) e^{ik_{lz}(2h_l - z_l')}\right]$$

$$+ \frac{1}{\left(1 - R_{\cup l}^{\mathrm{TM}} R_{\cap l}^{\mathrm{TM}} e^{2ik_{lz}h_l}\right)}$$

$$\left[\hat{v}(-k_{lz}) e^{-ik_{lz}z_l} + R_{\cap l}^{\mathrm{TM}} \hat{v}(k_{lz}) e^{ik_{lz}z_l}\right]$$

$$\left.\left[\hat{v}(-k_{lz}) e^{ik_{lz}z_l'} + R_{\cup l}^{\mathrm{TM}} \hat{v}(k_{lz}) e^{ik_{lz}(2h_l - z_l')}\right]\right\} \qquad (2b)$$

where z_l and z_l' are the local coordinates defined as $z_l = z + d_l$, $z_l' = z' + d_l$, and

$$\boldsymbol{k}_s = \hat{x}k_x + \hat{y}k_y$$

$$k_l^2 = k_s^2 + k_{lz}^2 \qquad k_s = |\boldsymbol{k}_s|$$

$$\hat{h}(\pm k_{lz}) = \frac{\hat{x}k_y - \hat{y}k_x}{k_s}$$

$$\hat{v}(\pm k_{lz}) = \mp \frac{k_{lz}\boldsymbol{k}_s}{k_l k_s} + \hat{z}\frac{k_s}{k_l}$$

$$\boldsymbol{r}_s = \hat{x}x + \hat{y}y \qquad \boldsymbol{r}_s' = \hat{x}x' + \hat{y}y'. \qquad (3)$$

In (2), $R_{\cup l}^{\mathrm{TM}}$ and $R_{\cup l}^{\mathrm{TE}}$ are the reflection coefficients of the TM mode and the TE mode at the upper boundary of the lth layer, and $R_{\cap l}^{\mathrm{TM}}$ and $R_{\cap l}^{\mathrm{TE}}$ are the reflection coefficients of the TM mode and the TE mode at the lower boundary of the lth layer. They can be obtained recursively as

$$R_{\cup l}^{\alpha} = \frac{R_{l(l-1)}^{\alpha} + R_{\cup(l-1)}^{\alpha} e^{2ik_{(l-1)z}h_{l+1}}}{1 + R_{l(l-1)}^{\alpha} R_{\cup(l-1)}^{\alpha} e^{2ik_{(l-1)z}h_{l-1}}}, \qquad \alpha = (\mathrm{TE}, \mathrm{TM}) \qquad (4a)$$

$$R_{\cap l}^{\alpha} = \frac{R_{l(l+1)}^{\alpha} + R_{\cap(l+1)}^{\alpha} e^{2ik_{(l+1)z}h_{l+1}}}{1 + R_{l(l+1)}^{\alpha} R_{\cap(l+1)}^{\alpha} e^{2ik_{(l+1)z}h_{l+1}}}, \qquad \alpha = (\mathrm{TE}, \mathrm{TM}) \qquad (4b)$$

where $R^{\alpha}_{l(l-1)}$ and $R^{\alpha}_{l(l+1)}$ are the Fresnel reflection coefficients of the α mode across the interfaces at $z=-d_{l-1}$ and $z=-d_l$, respectively. The explicit forms are

$$R^{\mathrm{TE}}_{l(l\pm1)}=\frac{k_{lz}-k_{(l\pm1)z}}{k_{lz}+k_{(l\pm1)z}} \qquad R^{\mathrm{TM}}_{l(l\pm1)}=\frac{\epsilon_{l\pm1}k_{lz}-\epsilon_l k_{(l\pm1)z}}{\epsilon_{l\pm1}k_{lz}+\epsilon_l k_{(l\pm1)z}}. \tag{5}$$

For our problem, only transverse currents $\boldsymbol{J}_s$ having no z component exist; the transverse electric field (to z) $\boldsymbol{E}_{ls}$ in layer (l) is thus given by

$$\boldsymbol{E}_{ls}(\bar{r})=i\omega\mu_l\iint_S d\boldsymbol{r}_s'\,\bar{\bar{G}}^T_{ll}(\boldsymbol{r},\boldsymbol{r}_s')\cdot\boldsymbol{J}_s(\boldsymbol{r}_s')\,dS' \tag{6}$$

where $\bar{\bar{G}}^T_{ll}(\boldsymbol{r},\boldsymbol{r}')$ is the (2×2) transverse (to z) part of the dyadic Green's function; it can be expressed in the $\boldsymbol{k}_s$ domain as

$$\bar{\bar{G}}^T_{ll}(\boldsymbol{r},\boldsymbol{r}')=\iint_{-\infty}^{\infty}d\boldsymbol{k}_s\,e^{i\boldsymbol{k}_s\cdot(\boldsymbol{r}_s-\boldsymbol{r}_s')}\bar{\bar{g}}^T_{ll}(\boldsymbol{k}_s,z,z') \tag{7}$$

where for $z>z'$,

$$\begin{aligned}\bar{\bar{g}}^T_{ll}(\boldsymbol{k}_s,z,z')&=\frac{i}{8\pi^2k_{lz}}\\&\cdot\left\{\frac{\left(e^{ik_{lz}z_l}+R^{\mathrm{TE}}_{\cup l}e^{ik_{lz}(2h_l-z_l)}\right)\left(e^{-ik_{lz}z_l'}+R^{\mathrm{TE}}_{\cap l}e^{ik_{lz}z_l'}\right)}{\left(1-R^{\mathrm{TE}}_{\cup l}R^{\mathrm{TE}}_{\cap l}e^{2ik_{lz}h_l}\right)}\right.\\&\cdot\frac{1}{k_s^2}\begin{bmatrix}k_y^2 & -k_xk_y\\ -k_xk_y & k_x^2\end{bmatrix}\\&+\frac{\left(e^{ik_{lz}z_l}-R^{\mathrm{TM}}_{\cup l}e^{ik_{lz}(2h_l-z_l)}\right)\left(e^{-ik_{lz}z_l'}-R^{\mathrm{TM}}_{\cap l}e^{ik_{lz}z_l'}\right)}{\left(1-R^{\mathrm{TM}}_{\cup l}R^{\mathrm{TM}}_{\cap l}e^{2ik_{lz}h_l}\right)}\\&\left.\cdot\frac{k_{lz}^2}{k_l^2k_s^2}\begin{bmatrix}k_x^2 & k_xk_y\\ k_xk_y & k_y^2\end{bmatrix}\right\}\end{aligned} \tag{8a}$$

and for $z<z'$,

$$\begin{aligned}\bar{\bar{g}}^T_{ll}(\boldsymbol{k}_s,z,z')&=\frac{i}{8\pi^2k_{lz}}\\&\cdot\left\{\frac{\left(e^{-ik_{lz}z_l}+R^{\mathrm{TE}}_{\cap l}e^{ik_{lz}z_l}\right)\left(e^{ik_{lz}z_l'}+R^{\mathrm{TE}}_{\cup l}e^{ik_{lz}(2h_l-z_l')}\right)}{\left(1-R^{\mathrm{TE}}_{\cup l}R^{\mathrm{TE}}_{\cap l}e^{2ik_{lz}h_l}\right)}\right.\\&\cdot\frac{1}{k_s^2}\begin{bmatrix}k_y^2 & -k_xk_y\\ -k_xk_y & k_x^2\end{bmatrix}\\&+\frac{\left(e^{-ik_{lz}z_l}-R^{\mathrm{TM}}_{\cap l}e^{ik_{lz}z_l}\right)\left(e^{ik_{lz}z_l'}-R^{\mathrm{TM}}_{\cup l}e^{ik_{lz}(2h_l-z_l')}\right)}{\left(1-R^{\mathrm{TM}}_{\cup l}R^{\mathrm{TM}}_{\cap l}e^{2ik_{lz}h_l}\right)}\\&\left.\cdot\frac{k_{lz}^2}{k_l^2k_s^2}\begin{bmatrix}k_x^2 & k_xk_y\\ k_xk_y & k_y^2\end{bmatrix}\right\}.\end{aligned} \tag{8b}$$

The transverse electric field can be expressed using Floquet harmonic representation in the y direction as

$$\boldsymbol{E}_{ls}(\bar{r})=i\omega\mu_l\int_{-\infty}^{\infty}dx'\int_{-p/2}^{p/2}dy'\,\bar{\bar{G}}^T_{llp}(\boldsymbol{r},\boldsymbol{r}_s')\cdot\boldsymbol{J}_s(\boldsymbol{r}_s') \tag{9}$$

where $\bar{\bar{G}}^T_{llp}(\boldsymbol{r},\boldsymbol{r}')$ is given by

$$\bar{\bar{G}}^T_{llp}(\boldsymbol{r},\boldsymbol{r}')=\frac{2\pi}{p}\sum_{n=-\infty}^{\infty}\int_{-\infty}^{\infty}dk_x\,e^{ik_x(x-x')}e^{ik_{yn}(y-y')}\cdot\bar{\bar{g}}^T_{ll}(k_x,k_{yn},z,z') \tag{10}$$

where $k_{yn}=k_{y0}+2n\pi/p$, and k_{y0} is the propagation constant of the dominant harmonic in the Floquet representation. We assume that we have M signal striplines and one crossing strip within one period. Thus, $\boldsymbol{J}_s$ can be expressed as

$$\boldsymbol{J}_s(x,y)=\begin{cases}\boldsymbol{J}_m(x,y), & x_m-w_m/2\leqslant x\leqslant x_m+w_m/2,\quad z=z_m\\ 0, & \text{elsewhere.}\end{cases} \tag{11}$$

Substituting (11) into (9), we have

$$\boldsymbol{E}_{ls}(\bar{r})=i\omega\mu_l(2\pi)^2\sum_{m=1}^{M+1}\sum_{n=-\infty}^{\infty}e^{ik_{yn}y}\cdot\int_{-\infty}^{\infty}dk_x\,e^{ik_xx}\bar{\bar{g}}^T_{ll}(k_x,k_{yn},z,z_m)\cdot\tilde{\boldsymbol{J}}_m(k_x,k_{yn}) \tag{12}$$

where

$$\tilde{\boldsymbol{J}}_m(k_x,k_{yn})=\frac{1}{2\pi p}\int_{-\infty}^{\infty}dx'e^{-ik_xx'}\cdot\int_{-p/2}^{p/2}dy'\,e^{-ik_{yn}y'}\boldsymbol{J}_m(x',y'). \tag{13}$$

The electric field $\boldsymbol{E}_{ls}$ given by (12) satisfies the boundary conditions at the interfaces between the dielectric layers of the stratified medium. Imposing the final boundary condition that the tangential electric fields vanish on the metallic surfaces of the signal striplines and the crossing strips, we obtain a set of vector integral equations for the current distribution on all the metallic strips. Thus, we have

$$\begin{aligned}&\sum_{m=1}^{M+1}\sum_{n=-\infty}^{\infty}e^{ik_{yn}y}\int_{-\infty}^{\infty}dk_x\,e^{ik_xx}\bar{\bar{g}}^T_{ll}(k_x,k_{yn},z,z_m)\\&\quad\cdot\tilde{\boldsymbol{J}}_m(k_x,k_{yn})=0, \qquad x_q-w_q/2\leqslant x\leqslant x_q+w_q/2,\\&\quad -p/2\leqslant y\leqslant p/2, \quad z=z_q, \quad q=1,\cdots,M\end{aligned} \tag{14a}$$

$$\begin{aligned}&\sum_{m=1}^{M+1}\sum_{n=-\infty}^{\infty}e^{ik_{yn}y}\int_{-\infty}^{\infty}dk_x\,e^{ik_xx}\bar{\bar{g}}^T_{ll}(k_x,k_{yn},z,z_m)\\&\quad\cdot\tilde{\boldsymbol{J}}_m(k_x,k_{yn})=0, \qquad -L_c/2\leqslant x\leqslant L_c/2,\\&\quad -w_c/2\leqslant y\leqslant w_c/2, \quad z=z_{M+1}\end{aligned} \tag{14b}$$

where (14a) satisfies the boundary condition on the M signal strips, and (14b) satisfies the boundary condition on

the crossing strip. The task is to solve this set of vector integral equations using the moment method to get the dispersion relation.

III. Numerical Solution for the Dispersion Relation

A. One Signal Stripline Loaded with Crossing Metallic Strips

In this section, we study the case of one signal stripline in the presence of periodical crossing strips as shown in Fig. 2. The signal stripline and the crossing strips are located in a dielectric layer bounded by two ground planes and placed, respectively, at $z = z_1$ and $z = z_2$.

To apply the moment method, we choose an appropriate set of basis functions to represent the surface current $\boldsymbol{J}_1(x, y)$ and $\boldsymbol{J}_2(x, y)$ as

$$\boldsymbol{J}_1(x, y) = \hat{x} \sum_{j=-N_1}^{N_2} a_j f_{1j}(x, y) + \hat{y} \sum_{j=-N_1}^{N_2} b_j f_{2j}(x, y) \tag{15a}$$

$$\boldsymbol{J}_2(x, y) = \hat{x} \sum_{j=1}^{N_3} c_j f_{3j}(x, y) + \hat{y} \sum_{j=0}^{N_4} d_j f_{4j}(x, y) \tag{15b}$$

where $\boldsymbol{J}_1(x, y)$ is the surface current on the signal stripline; $\boldsymbol{J}_2(x, y)$ is the surface current on the crossing strip; a_j, b_j, c_j, and d_j are the expansion coefficients; and $f_{1j}(x, y)$, $f_{2j}(x, y)$, $f_{3j}(x, y)$, and $f_{4j}(x, y)$ are the basis functions. The explicit forms of the basis functions are as follows:

$$f_{1j}(x, y) = P_1(x, w_1) e^{ik_{yj}y} \tag{16a}$$

$$f_{2j}(x, y) = T_0(x, w_1) e^{ik_{yj}y} \tag{16b}$$

$$f_{3j}(x, y) = P_j(x, L_c)(p/2\pi) T_0(y, w_c) \tag{16c}$$

$$f_{4j}(x, y) = T_j(x, L_c) Q(y, w_c) \tag{16d}$$

where

$$P_j(\xi, \eta) = \begin{cases} (1/\eta)\sin(2j\pi\xi/\eta), \\ \qquad -\eta/2 \leqslant \xi \leqslant \eta/2 \\ 0, \qquad \text{elsewhere} \end{cases} \tag{17a}$$

$$Q(\xi, \eta) = \begin{cases} (p/2\pi\eta)\cos(\pi\xi/\eta), \\ \qquad -\eta/2 \leqslant \xi \leqslant \eta/2 \\ 0, \qquad \text{elsewhere} \end{cases} \tag{17b}$$

$$T_j(\xi, \eta) = \begin{cases} \cos(2j\pi\xi/\eta)\Big/\sqrt{(\eta/2)^2 - \xi^2}, \\ \qquad -\eta/2 \leqslant \xi \leqslant \eta/2 \\ 0, \qquad \text{elsewhere.} \end{cases} \tag{17c}$$

The surface current on the signal stripline is basically of the traveling wave type. Due to the periodic loading, the basis functions on the signal stripline are chosen as a superposition of space harmonic modes. On the crossing strips, the surface current is basically of the standing wave type, and the phase variation along the y direction on the crossing strips can be neglected.

Let $\tilde{P}_j(k_x, \eta)$, $\tilde{Q}(k_{yn}, \eta)$, and $\tilde{T}_j(k_x, \eta)$ be the Fourier transforms of $P_j(x, \eta)$, $Q(y, \eta)$, and $T_j(x, \eta)$, respectively;

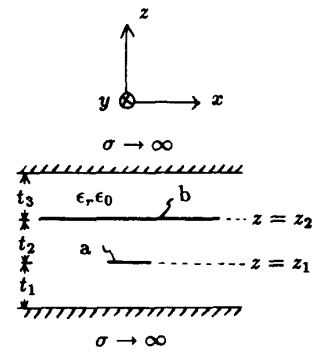

a signal strip b crossing strip

Fig. 2. Geometrical configuration of one signal stripline periodically loaded with crossing strips embedded in a one-layer medium.

we have

$$\begin{aligned} \tilde{P}_j(k_x, \eta) &= \frac{1}{2\pi}\int_{-\eta/2}^{\eta/2} dx e^{-ik_x x} P_j(x, \eta) \\ &= i\frac{j(-1)^{j+1}\sin(k_x\eta/2)}{2\left[(k_x\eta/2)^2 - (j\pi)^2\right]} \\ &= -\tilde{P}_j(-k_x, \eta) \end{aligned} \tag{18a}$$

$$\begin{aligned} \tilde{Q}(k_{yn}, \eta) &= \frac{1}{p}\int_{-\eta/2}^{\eta/2} dy e^{-ik_{yn}y} Q(y, \eta) \\ &= -\frac{\cos(k_{yn}\eta/2)}{(k_{yn}\eta)^2 - \pi^2} \\ &= \tilde{Q}(-k_{yn}, \eta) \end{aligned} \tag{18b}$$

$$\begin{aligned} \tilde{T}_j(k_x, \eta) &= \frac{1}{2\pi}\int_{-\eta/2}^{\eta/2} dx e^{-ik_x x} T_j(x, \eta) \\ &= \frac{1}{4}\left[J_0(k_x\eta/2 - j\pi) + J_0(k_x\eta/2 + j\pi)\right] \\ &= \tilde{T}_j(-k_x, \eta) \end{aligned} \tag{18c}$$

where $J_0(\alpha)$ is the Bessel function of the zeroth order, $\tilde{P}_j(k_x, \eta)$ is an odd function of k_x, $\tilde{T}_j(k_x, \eta)$ is an even function of k_x, and $\tilde{Q}(k_{yn}, \eta)$ is an even function of k_{yn}. When $k_x\eta/2$ approaches $\pm j\pi$, $\tilde{P}_j(k_x, \eta)$ approaches $\pm 1/(4\pi i)$; when $k_{yn}\eta$ approaches $\pm\pi$, $\tilde{Q}(k_{yn}, \eta)$ approaches $1/(4\pi)$.

With these basis functions, the Fourier transform of the surface current $\tilde{\boldsymbol{J}}_m(k_x, k_{yn})$ can be derived as

$$\begin{aligned} \tilde{\boldsymbol{J}}_1(k_x, k_{yn}) &= \hat{x} \sum_{j=-N_1}^{N_2} a_j F_{1j}(k_x, k_{yn}) \\ &\quad + \hat{y} \sum_{j=-N_1}^{N_2} b_j F_{2j}(k_x, k_{yn}) \end{aligned} \tag{19a}$$

$$\tilde{\boldsymbol{J}}_2(k_x, k_{yn}) = \hat{x} \sum_{j=1}^{N_3} c_j F_{3j}(k_x, k_{yn}) + \hat{y} \sum_{j=0}^{N_4} d_j F_{4j}(k_x, k_{yn}) \tag{19b}$$

where $F_{ij}(k_x, k_{yn})$ is the Fourier transform of $f_{ij}(x, y)$, $i = 1,2,3,4$. The explicit forms are

$$F_{1j}(k_x, k_{yn}) = \delta_{jn}\tilde{P}_1(k_x, w_1) \tag{20a}$$

$$F_{2j}(k_x, k_{yn}) = \delta_{jn}\tilde{T}_0(k_x, w_1) \tag{20b}$$

$$F_{3j}(k_x, k_{yn}) = \tilde{T}_0(k_{yn}, w_c)\tilde{P}_j(k_x, L_c) \tag{20c}$$

$$F_{4j}(k_x, k_{yn}) = \tilde{Q}(k_{yn}, w_c)\tilde{T}_j(k_x, L_c) \tag{20d}$$

where δ_{jn} is the Kronecker delta function. Substituting (20) into (14), we have

$$\sum_{n=-\infty}^{\infty} e^{ik_{yn}y}\int_{-\infty}^{\infty} dk_x e^{ik_x x}\bar{\bar{g}}_{ll}^{T}(k_x, k_{yn}, z_1, z_1)$$
$$\cdot\left[\hat{x}\sum_{j=-N_1}^{N_2} a_j F_{1j}(k_x, k_{yn}) + \hat{y}\sum_{j=-N_1}^{N_2} b_j F_{2j}(k_x, k_{yn})\right]$$
$$+ \bar{\bar{g}}_{ll}^{T}(k_x, k_{yn}, z_1, z_2)$$
$$\cdot\left[\hat{x}\sum_{j=1}^{N_3} c_j F_{3j}(k_x, k_{yn}) + \hat{y}\sum_{j=0}^{N_4} d_j F_{4j}(k_x, k_{yn})\right] = 0,$$
$$-w_1/2 \le x \le w_1/2,$$
$$-p/2 \le y \le p/2, \quad z = z_1 \tag{21a}$$

$$\sum_{n=-\infty}^{\infty} e^{ik_{yn}y}\int_{-\infty}^{\infty} dk_x e^{ik_x x}\bar{\bar{g}}_{ll}^{T}(k_x, k_{yn}, z_2, z_1)$$
$$\cdot\left[\hat{x}\sum_{j=-N_1}^{N_2} a_j F_{1j}(k_x, k_{yn}) + \hat{y}\sum_{j=-N_1}^{N_2} b_j F_{2j}(k_x, k_{yn})\right]$$
$$+ \bar{\bar{g}}_{ll}^{T}(k_x, k_{yn}, z_2, z_2)$$
$$\cdot\left[\hat{x}\sum_{j=1}^{N_3} c_j F_{3j}(k_x, k_{yn}) + \hat{y}\sum_{j=0}^{N_4} d_j F_{4j}(k_x, k_{yn})\right] = 0,$$
$$-L_c/2 \le x \le L_c/2,$$
$$-w_c/2 \le y \le w_c/2, \quad z = z_2. \tag{21b}$$

Applying Galerkin's method, we choose $\hat{x}e^{-ik_{yk}y}P_1(x, w_1)$ $(k = -N_1, \cdots, N_2)$ and $\hat{y}e^{-ik_{yk}y}T_0(x, w_1)$ $(k = -N_1, \cdots, N_2)$ as testing functions for the signal stripline. Taking the inner product with (21a), we obtain $2(N_1 + N_2 + 1)$ equations. Similarly, taking the inner product of $\hat{x}f_{3i}(x, y)$ $(i = 1, \cdots, N_3)$ and $\hat{y}f_{4k}(x, y)$ $(k = 0, \cdots, N_4)$ with (21b), we obtain another $N_3 + N_4 + 1$ equations.

After arrangement, we obtain the following matrix equation:

$$\begin{bmatrix} Z_{i,j}^{(1,1)} & Z_{i,j}^{(1,2)} & Z_{i,j}^{(1,3)} & Z_{i,j}^{(1,4)} \\ Z_{i,j}^{(2,1)} & Z_{i,j}^{(2,2)} & Z_{i,j}^{(2,3)} & Z_{i,j}^{(2,4)} \\ Z_{i,j}^{(3,1)} & Z_{i,j}^{(3,2)} & Z_{i,j}^{(3,3)} & Z_{i,j}^{(3,4)} \\ Z_{i,j}^{(4,1)} & Z_{i,j}^{(4,2)} & Z_{i,j}^{(4,3)} & Z_{i,j}^{(4,4)} \end{bmatrix}\begin{bmatrix} a_j \\ b_j \\ c_j \\ d_j \end{bmatrix} = 0. \tag{22}$$

Each entity $Z_{i,j}^{(r,q)}$ in (22) is a submatrix; the explicit form of the elements is

$$Z_{i,j}^{(r,q)}(\omega, k_y) = \sum_{n=-\infty}^{\infty}\int_{-\infty}^{\infty} dk_x S_{i,j}^{(r,q)}(k_x, k_{yn}) \tag{23}$$

with

$$S_{i,j}^{(r,q)}(k_x, k_{yn}) = F_{ri}(-k_x, -k_{yn})g_{ll}^{\alpha\beta}(k_x, k_{yn}, z_t, z_m) \cdot F_{qj}(k_x, k_{yn}) \tag{24}$$

where

$$z_t = \begin{cases} z_1 & \text{for } r = 1,2 \\ z_2 & \text{for } r = 3,4 \end{cases} \qquad z_m = \begin{cases} z_1 & \text{for } q = 1,2 \\ z_2 & \text{for } q = 3,4 \end{cases} \tag{25a}$$

$$\alpha = \begin{cases} x & \text{for } r = 1,3 \\ y & \text{for } r = 2,4 \end{cases} \qquad \beta = \begin{cases} x & \text{for } q = 1,3 \\ y & \text{for } q = 2,4. \end{cases} \tag{25b}$$

The determinantal equation for the propagation constant k_{y0} can be solved by setting the determinant of the coefficient matrix of (22) equal to zero:

$$\det\left[Z(\omega, k_{y0})\right] = 0. \tag{26}$$

B. Two Symmetrical Signal Striplines Loaded with Crossing Strips

In this section, we consider the case where two identical signal striplines of width w_1 are located symmetrically at $(\pm x_c, z_1)$ as shown in Fig. 3.

For the even modes, $J_{mx}(x, y)$ is an odd function of x, and $J_{my}(x, y)$ is an even function of x. Therefore, the surface currents can be expanded as

$$\boldsymbol{J}_1(x, y) = \hat{x}\sum_{j=-N_1}^{N_2} a_j f_{1j}^{(e)}(x, y) + \hat{y}\sum_{j=-N_1}^{N_2} b_j f_{2j}^{(e)}(x, y) \tag{27a}$$

$$\boldsymbol{J}_2(x, y) = \hat{x}\sum_{j=1}^{N_3} c_j f_{3j}^{(e)}(x, y) + \hat{y}\sum_{j=0}^{N_4} d_j f_{4j}^{(e)}(x, y) \tag{27b}$$

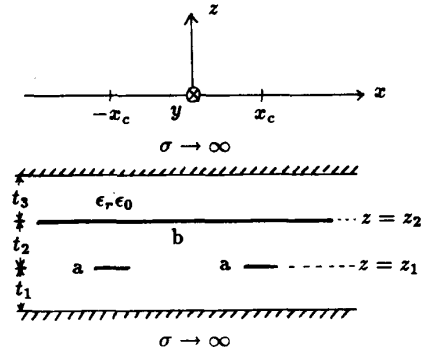

a signal strip b crossing strip

Fig. 3. Geometrical configuration of two signal striplines periodically loaded with crossing strips embedded in a one-layer medium.

where the basis functions are

$$f_{1j}^{(e)}(x,y) = \left[P_1(x-x_c,w_1)+P_1(x+x_c,w_1)\right]e^{ik_{yj}y} \tag{28a}$$

$$f_{2j}^{(e)}(x,y) = \left[T_0(x-x_c,w_1)+T_0(x+x_c,w_1)\right]e^{ik_{yj}y} \tag{28b}$$

$$f_{3j}^{(e)}(x,y) = P_j(x,L_c)(p/2\pi)T_0(y,w_c) \tag{28c}$$

$$f_{4j}^{(e)}(x,y) = T_j(x,L_c)Q(y,w_c). \tag{28d}$$

Following the same procedure as in the case of one signal stripline by applying the Galerkin method, a determinantal equation similar to (26) is obtained.

For the odd modes, $J_{mx}(x,y)$ is an even function of x, and $J_{my}(x,y)$ is an odd function of x. Therefore, the surface currents are expanded as

$$\boldsymbol{J}_1(x,y) = \hat{x}\sum_{j=-N_1}^{N_2} a_j f_{1j}^{(o)}(x,y) + \hat{y}\sum_{j=-N_1}^{N_2} b_j f_{2j}^{(o)}(x,y) \tag{29a}$$

$$\boldsymbol{J}_2(x,y) = \hat{x}\sum_{j=1}^{N_3} c_j f_{3j}^{(o)}(x,y) + \hat{y}\sum_{j=0}^{N_4} d_j f_{4j}^{(o)}(x,y) \tag{29b}$$

where the basis functions are

$$f_{1j}^{(o)}(x,y) = \left[P_1(x-x_c,w_1)-P_1(x+x_c,w_1)\right]e^{ik_{yj}y} \tag{30a}$$

$$f_{2j}^{(o)}(x,y) = \left[T_0(x-x_c,w_1)-T_0(x+x_c,w_1)\right]e^{ik_{yj}y} \tag{30b}$$

$$f_{3j}^{(o)}(x,y) = U_j(x,L_c)(p/2\pi)T_0(y,w_c) \tag{30c}$$

$$f_{4j}^{(o)}(x,y) = V_j(x,L_c)Q(y,w_c) \tag{30d}$$

where

$$U_j(\xi,\eta) = \begin{cases} (1/\eta)\cos\left[(2j-1)\pi\xi/\eta\right], \\ \qquad -\eta/2 \leqslant \xi \leqslant \eta/2 \\ 0, \qquad \text{elsewhere} \end{cases} \tag{31a}$$

$$V_j(\xi,\eta) = \begin{cases} \sin\left[(2j-1)\pi\xi/\eta\right]/\sqrt{(\eta/2)^2-\xi^2}, \\ \qquad -\eta/2 \leqslant \xi \leqslant \eta/2 \\ 0, \qquad \text{elsewhere.} \end{cases} \tag{31b}$$

Let $\tilde{U}_j(k_x,\eta)$ and $\tilde{V}_j(k_x,\eta)$ be the Fourier transform of $U_j(x,\eta)$ and $V_j(x,\eta)$; then

$$\tilde{U}_j(k_x,\eta) = \frac{(2j-1)(-1)^j\cos(k_x\eta/2)}{(k_x\eta)^2-\left[(2j-1)\pi\right]^2} = \tilde{U}_j(-k_x,\eta) \tag{32a}$$

$$\begin{aligned}\tilde{V}_j(k_x,\eta) &= \frac{1}{4i}\left[J_0(k_x\eta/2-(j-1/2)\pi)\right. \\ &\quad \left. - J_0(k_x\eta/2+(j-1/2)\pi)\right] \\ &= -\tilde{V}_j(-k_x,\eta).\end{aligned} \tag{32b}$$

When $k_x\eta/2$ approaches $\pm(j-1/2)\pi$, $\tilde{U}_j(k_x,\eta)$ approaches $1/(4\pi)$.

C. One Signal Stripline Loaded with Crossing Strips of Infinite Length

In this section, we consider the case where one signal line is loaded by infinitely long crossing strips as shown in Fig. 2 with $L_c \to \infty$. When the crossing strips are very long such that reflections from the ends can be neglected, we can assume traveling waves along it. So, we investigate the possibility of the existence of such a mode of operation and its effect on the propagation characteristics of the signal line.

The surface current on the signal strip is of the same form as in the case discussed in subsection A of finite crossing strips. For the crossing strips, we choose traveling wave basis functions [9], [10] and some local basis functions on the center to account for the effect of the presence of the signal line. Hence, the surface currents are expanded as

$$\boldsymbol{J}_1(x,y) = \hat{x}\sum_{j=-N_1}^{N_2} a_j f_{1j}^{(t)}(x,y) + \hat{y}\sum_{j=-N_1}^{N_2} b_j f_{2j}^{(t)}(x,y) \tag{33a}$$

$$\boldsymbol{J}_2(x,y) = \hat{x}\sum_{j=1}^{N_3} c_j f_{3j}^{(t)}(x,y) + \hat{y}\sum_{j=0}^{N_4} d_j f_{4j}^{(t)}(x,y) \tag{33b}$$

where the basis functions $f_{1j}^{(t)}(x,y)$ and $f_{2j}^{(t)}(x,y)$ are the same as $f_{1j}(x,y)$ and $f_{2j}(x,y)$, respectively. The functional forms of $f_{3j}^{(t)}(x,y)$ and $f_{4j}^{(t)}(x,y)$ are

$$f_{3j}^{(t)}(x,y) = \begin{cases} \left[R_j(x,h)-R_j(-x,h)\right](p/2\pi)T_0(y,w_c), \\ \qquad 1 \leqslant j \leqslant N_3-1 \\ \left[-S_m(k_e x-\pi/2)+iS_m(k_e x)\right. \\ \left.+S_m(-k_e x-\pi/2)-iS_m(-k_e x)\right] \\ (p/2\pi)T_0(y,w_c), \qquad j=N_3 \end{cases} \tag{34a}$$

$$f_{4j}^{(t)}(x,y) = \begin{cases} R_0(x,h)Q(y,w_c), \\ \qquad j=0 \\ \left[R_j(x,h)+R_j(-x,h)\right]Q(y,w_c), \\ \qquad 1 \leqslant j \leqslant N_4-1 \\ \left[-S_m(k_e x-\pi/2)+iS_m(k_e x)\right. \\ \left.-S_m(-k_e x-\pi/2)+iS_m(-k_e x)\right]Q(y,w_c) \\ \qquad j=N_4 \end{cases} \tag{34b}$$

where k_e is assumed to be the propagation constant of a single crossing strip of infinite length in the absence of the signal line, $R_j(x,h)$ is the local basis function with width $2h$, and $S_m(\xi)$ is the traveling wave basis function with

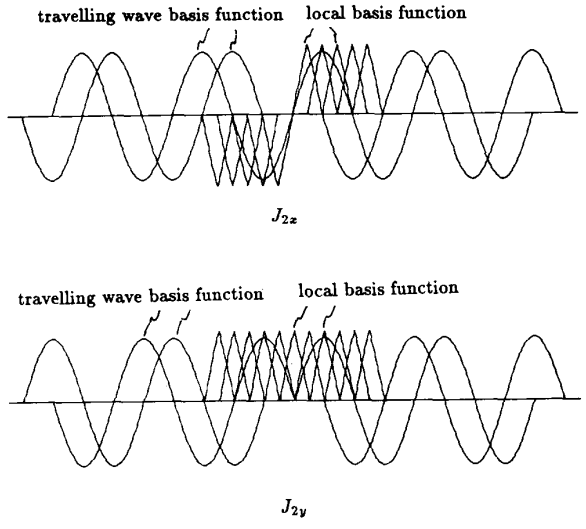

Fig. 4. The basis functions used for infinitely long crossing strips, $m = 4$, $N_3 = N_4 = 6$.

$m/2$ periods as shown in Fig. 4. The explicit forms are

$$R_j(x,h) = \begin{cases} \sin k_e(h - |x - jh|)/\sin k_e h, \\ \qquad (j-1)h \leqslant x \leqslant (j+1)h \\ 0, \quad \text{elsewhere} \end{cases} \tag{35a}$$

$$S_m(\xi) = \begin{cases} \sin\xi, & 0 \leqslant \xi \leqslant m\pi \\ 0, & \text{elsewhere.} \end{cases} \tag{35b}$$

It will be shown that only a finite number of periods of the traveling wave basis functions are sufficient for the convergence of the solution. Any increase in the number of periods of these basis functions will have a negligible effect on the numerical results.

Let $\tilde{R}_j(k_x, w)$ and $\tilde{S}_m(k_x)$ be the Fourier transform of $R_j(x,h)$ and $S_m(\xi)$; then

$$\tilde{R}_j(k_x,h) = -\frac{k_e e^{-ik_x jh}(\cos k_x h - \cos k_e h)}{\pi \sin k_e h (k_x^2 - k_e^2)} \tag{36a}$$

$$\tilde{S}_m(k_x) = \frac{k_e}{2\pi(k_x^2 - k_e^2)}\left[(-1)^m e^{-i(m\pi/k_e)k_x} - 1\right]. \tag{36b}$$

When the value of k_x approaches $\pm k_e$, $\tilde{R}_j(k_x,h)$ and $\tilde{S}_m(k_x)$ approach $(h/2\pi)e^{\mp ik_e jh}$ and $\mp im/4k_e$, respectively.

With these basis functions, the Fourier transform of the surface current $\tilde{J}_m(k_x, k_{yn})$ can be derived as

$$\tilde{J}_1(k_x,k_{yn}) = \hat{x}\sum_{j=-N_1}^{N_2} a_j F_{1j}^{(t)}(k_x,k_{yn}) + \hat{y}\sum_{j=-N_1}^{N_2} b_j F_{2j}^{(t)}(k_x,k_{yn}) \tag{37a}$$

$$\tilde{J}_2(k_x,k_{yn}) = \hat{x}\sum_{j=1}^{N_3} c_j F_{3j}^{(t)}(k_x,k_{yn}) + \hat{y}\sum_{j=0}^{N_4} d_j F_{4j}^{(t)}(k_x,k_{yn}) \tag{37b}$$

where $F_{ij}^{(t)}(k_x, k_{yn})$ is the Fourier transform of $f_{ij}^{(t)}(x,y)$, $i = 1,2,3,4$. The explicit forms are

$$F_{1j}^{(t)}(k_x,k_{yn}) = \delta_{jn}\tilde{P}_1(k_x,w_1) \tag{38a}$$

$$F_{2j}^{(t)}(k_x,k_{yn}) = \delta_{jn}\tilde{T}_0(k_x,w_1) \tag{38b}$$

$$F_{3j}^{(t)}(k_x,k_{yn}) = \tilde{T}_0(k_{yn},w_c)\tilde{A}_{3j}(k_x) \tag{38c}$$

$$F_{4j}^{(t)}(k_x,k_{yn}) = \tilde{Q}(k_{yn},w_c)\tilde{A}_{4j}(k_x) \tag{38d}$$

where

$$\tilde{A}_{3j}(k_x) = \begin{cases} 2\tilde{R}_j^{(o)}(k_x,h), \\ \qquad 1 \leqslant j \leqslant N_3 - 1 \\ k_e\left[\pi(k_x^2 - k_e^2)\right]^{-1}\left[(-1)^m \right. \\ \cdot i\sin\left[k_x\pi(m+1/2)/k_e\right] \\ +(-1)^m \sin(m\pi k_x/k_e) \\ \left. -i\sin(k_x\pi/2k_e)\right], \\ \qquad j = N_3 \end{cases} \tag{39a}$$

$$\tilde{A}_{4j}(k_x) = \begin{cases} \tilde{R}_0^{(e)}(k_x,h), \\ \qquad j = 0 \\ 2\tilde{R}_j^{(e)}(k_x,h), \\ \qquad 1 \leqslant j \leqslant N_4 - 1 \\ k_e\left[\pi(k_x^2 - k_e^2)\right]^{-1}\left[-(-1)^m \right. \\ \cdot\cos\left[k_x\pi(m+1/2)/k_e\right] \\ +i(-1)^m \\ \left. \cdot\cos(m\pi k_x/k_e) + \cos(k_x\pi/2k_e) - i\right], \\ \qquad j = N_4 \end{cases}$$

where $\tilde{R}_j^{(e)}(k_x,h)$ and $\tilde{R}_j^{(o)}(k_x,h)$ are the even part and the odd part of $\tilde{R}_j(k_x,h)$, respectively. It is observed that $\tilde{A}_{3j}(-k_x) = -\tilde{A}_{3j}(k_x)$, and $\tilde{A}_{4j}(-k_x) = \tilde{A}_{4j}(k_x)$.

Applying the Galerkin procedure with the following testing functions:

$$w_{1j}(x,y) = P_1(x,w_1)e^{-ik_{yj}y} \tag{40a}$$

$$w_{2j}(x,y) = T_0(x,w_1)e^{-ik_{yj}y} \tag{40b}$$

$$w_{3j}(x,y) = R_j(x,h)(p/2\pi)T_0(y,w_c) \tag{40c}$$

$$w_{4j}(x,y) = R_j(x,h)Q(y,w_c) \tag{40d}$$

the matrix eigenvalue equation is obtained.

IV. Numerical Results and Discussion

By utilizing the symmetry properties of the dyadic Green's function, the basis functions, and the testing functions, each matrix element in (22) can be reduced to an integral over $0 \leqslant k_x < \infty$. In computing the integrals (23) numerically, the path of integration in the complex k_x

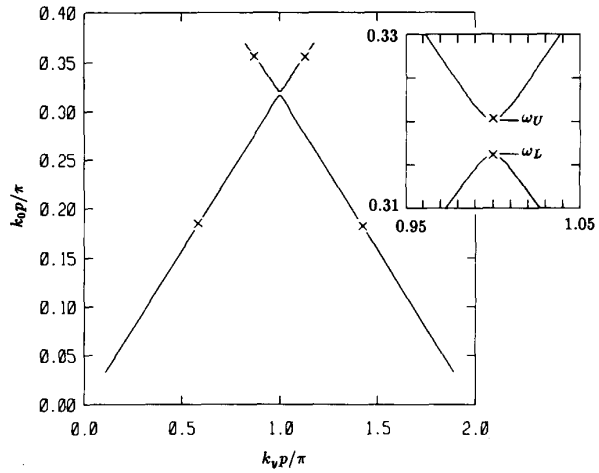

Fig. 5. Dispersion relation of one signal stripline periodically loaded with crossing strips of finite length, $\epsilon_r = 10$, $t_1 = t_2 = t_3 = 0.2$ mm, $p = 0.5$ mm, $w_1 = w_c = 0.125$ mm, $L_c = 2.3$ mm, $N_1 = 1$, $N_2 = 0$, $N_3 = 4$, $N_4 = 3$, $\times$: $N_1 = 1$, $N_2 = 0$, $N_3 = 6$, $N_4 = 5$, ω_U: upper bound of the first stopband, ω_L: lower bound of the first stopband.

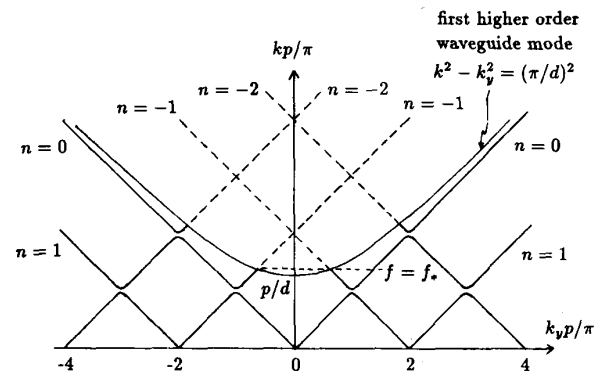

Fig. 6. Interaction of Floquet modes with TE_1 (TM_1) parallel-plate waveguide mode, $k = \omega\sqrt{\mu_0\epsilon_0\epsilon_r}$, $d = t_1 + t_2 + t_3$.

plane is deformed below the real axis to avoid the poles corresponding to the waveguide modes [11].

Fig. 5 shows the dispersion relation for a single signal line with crossing strips. Numerical computations were performed with two different numbers of basis functions, and the results were found to be the same up to three decimal points. The basis functions used are given by (15). For $L_c = 2.3$ mm, the first stopband occurs in the frequency range when $0.3162 < k_0p/\pi < 0.3203$.

Fig. 6 shows the interaction of an $n = -1$ Floquet mode with a TE_1 (TM_1) parallel-plate waveguide mode. For frequencies above f_*, k_y starts to have a large imaginary part, giving rise to a higher order stopband. However, we are interested in operating frequencies where k_y is real within the passbands below f_*, and thus the region above f_* is of no practical importance.

Next, the effects of crossing strip length L_c on the lower and upper frequency bounds of the stopband are investigated. The normalized frequency for the two bounds of the

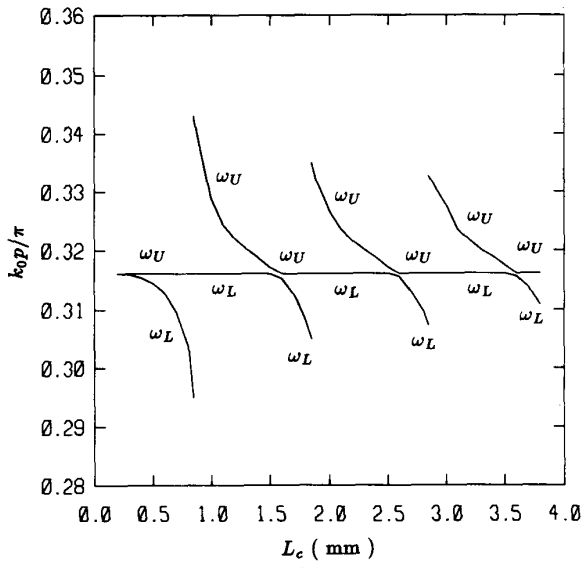

(a)

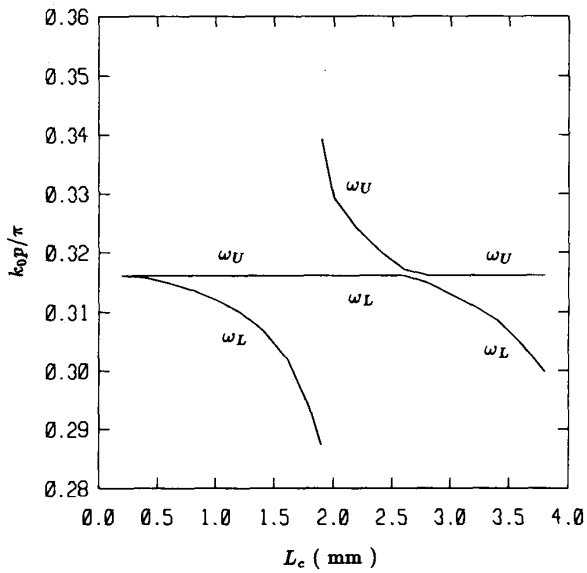

(b)

Fig. 7. (a) The effects of L_c on the upper and lower bounds of the stopband, $\epsilon_r = 10$, $t_1 = t_2 = t_3 = 0.2$ mm, $p = 0.5$ mm, $w_1 = w_c = 0.125$ mm, $N_1 = 1$, $N_2 = 0$, $N_3 = 5$, $N_4 = 4$. (b) The effects of L_c on the upper and lower bounds of the stopband, $\epsilon_r = 10$, $t_1 = t_2 = t_3 = 0.2$ mm, $p = 1.0$ mm, $w_1 = w_c = 0.125$ mm, $N_1 = 1$, $N_2 = 0$, $N_3 = 5$, $N_4 = 4$.

stopband is presented as a function of L_c. The result for $p = 0.5$ mm is plotted in Fig. 7(a). It is observed that both bounds of the stopband are very sensitive to the crossing strip length L_c. This behavior is repeated when L_c changes by an approximately integral number of wavelengths. This can be explained in the following way: The crossing strips behave like open-circuited stubs periodically loading the signal line. The crossing strips will have capacitive or inductive behavior depending on its length. At a certain length of crossing strips, the behavior switches from being

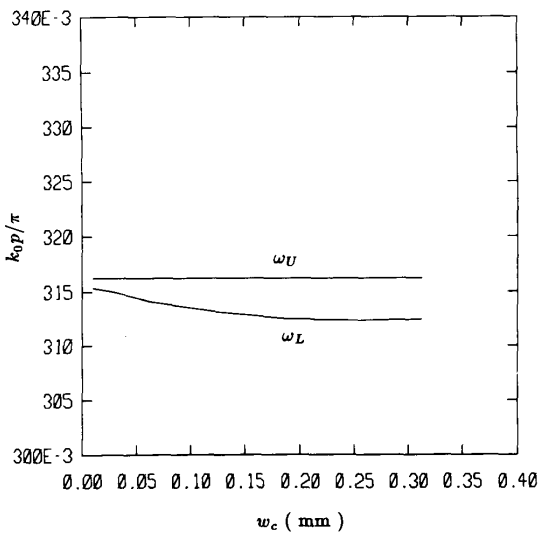

Fig. 8. The effects of w_c on the upper and lower bounds of the stopband, $\epsilon_r = 10$, $t_1 = t_2 = t_3 = 0.2$ mm, $p = 0.5$ mm, $w_1 = 0.125$ mm, $L_c = 2.7$ mm, $N_1 = 1$, $N_2 = 0$, $N_3 = 4$, $N_4 = 3$.

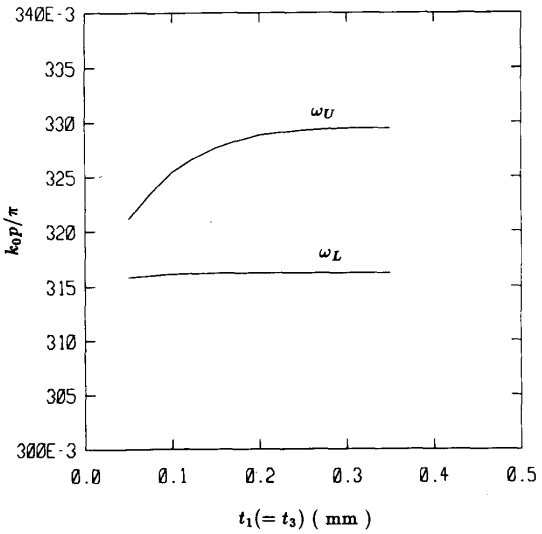

Fig. 9. The effects of t_1 and t_3 on the upper and lower bounds of the stopband, $\epsilon_r = 10$, $t_2 = 0.2$ mm, $p = 0.5$ mm, $w_1 = w_c = 0.125$ mm, $L_c = 1.0$ mm, $N_1 = 1$, $N_2 = 0$, $N_3 = 2$, $N_4 = 1$.

inductive (or capacitive) to capacitive (or inductive). This switching occurs at $L_c \approx n\lambda_1$, where λ_1 is the wavelength in the dielectric medium calculated at the center frequency. At these lengths, the stopbands become very wide.

In Fig. 7(b), the normalized frequency of the bounds of the stopband is plotted as a function of L_c with the period $p = 1.0$ mm. Behavior similar to that in Fig. 7(a) is observed, but the values of L_c at which the switching of frequency occurs are doubled.

In Fig. 8, the effects of the crossing strip width w_c on the stopband frequency bounds are investigated. The normalized frequency at the bounds of the stopband is presented for $L_c = 2.7$ mm. As the crossing strip width becomes smaller, the stopband becomes narrower.

In Fig. 9, we investigate the effect of the separations t_1 and t_3 on the stopband while keeping t_2 constant. It is observed that the stopband becomes smaller when the separation is decreased, and when the separation is larger than 0.2 mm, the upper frequency bound of the stopband reaches a constant.

In Fig. 10, the bounds of the first stopband are plotted as a function of the distance t_2 while fixing the separation $t_1 = t_3 =$ constant. It is observed that for $L_c = 1.0$ mm, the separation t_2 affects the upper bound of the first stopband significantly.

Fig. 11 shows the case of two coupled signal striplines in the presence of periodic crossing strips of finite length. The frequency bounds of the stopband are presented in Fig. 11(a) and (b) for the even mode and the odd mode, respectively, with $p = 0.5$ mm and $L_c = 1.7$ mm. The basis functions used are given by (27) and (29) for the even and the odd mode, respectively. When the separation becomes larger than L_c, the stopband width of the even mode approaches zero, but the stopband width of the odd mode is still finite. This is because the odd mode has stronger coupling between two signal lines than the even mode.

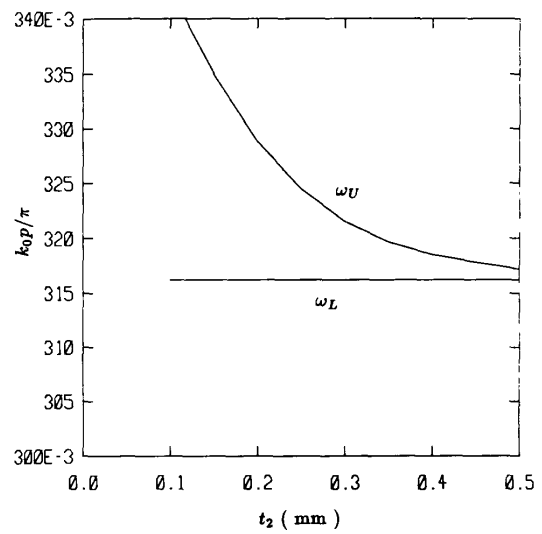

Fig. 10. The effects of t_2 on the upper and lower bounds of the stopband, $\epsilon_r = 10$, $t_1 = t_3 = 0.2$ mm, $p = 0.5$ mm, $w_1 = w_c = 0.125$ mm, $L_c = 1.0$ mm, $N_1 = 1$, $N_2 = 0$, $N_3 = 2$, $N_4 = 1$.

Fig. 12 shows the dispersion relation of a single stripline in the presence of crossing strips of infinite length. The basis functions used are given by (33). We choose the traveling wave basis functions to have three periods. The results using seven periods are also shown for comparison,

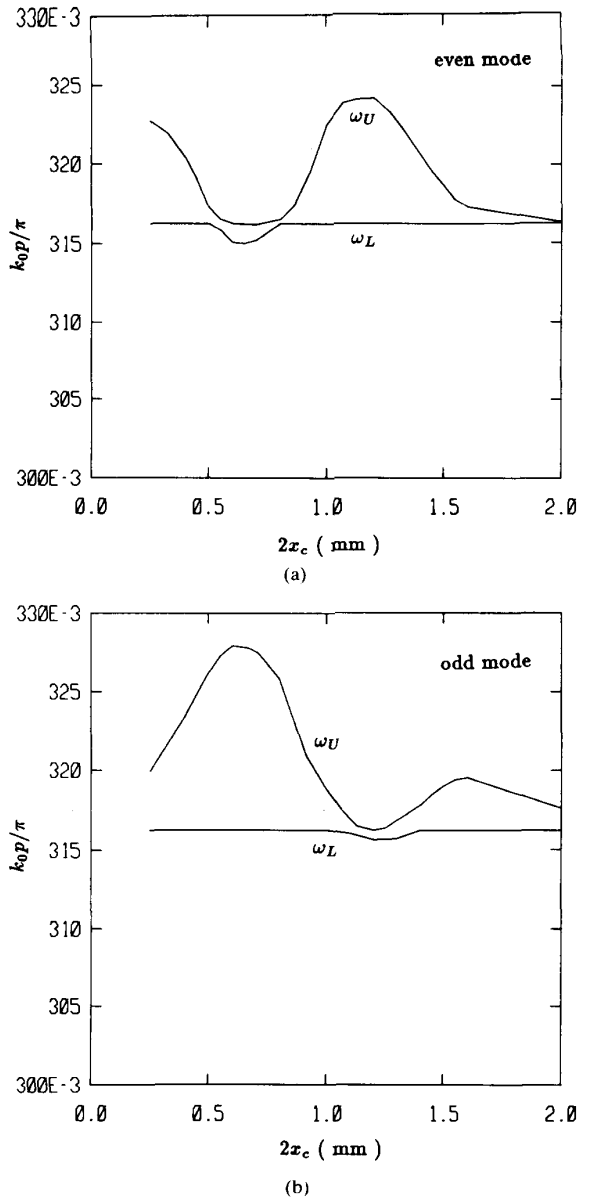

Fig. 11. (a) The effects of x_c on the upper and lower bounds of the stopband, for two signal striplines, $\epsilon_r = 10$, $t_1 = t_2 = t_3 = 0.2$ mm, $p = 0.5$ mm, $w_1 = w_c = 0.125$ mm, $L_c = 1.7$ mm, $N_1 = 1$, $N_2 = 0$, $N_3 = 3$, $N_4 = 2$. (b) The effects of x_c on the upper and lower bounds of the stopband, for two signal striplines, $\epsilon_r = 10$, $t_1 = t_2 = t_3 = 0.2$ mm, $p = 0.5$ mm, $w_1 = w_c = 0.125$ mm, $L_c = 1.7$ mm, $N_1 = 1$, $N_2 = 0$, $N_3 = 3$, $N_4 = 2$.

and it is found that the traveling wave basis function of three periods is sufficient. The imaginary part of the propagation constant is approximately a linear function of frequency, and the magnitude can be as high as 1 percent of the real part. This is due to the assumption that the surface current along the crossing strips is a traveling wave. Part of the power along the signal line couples to the crossing strips, exciting a traveling wave surface current

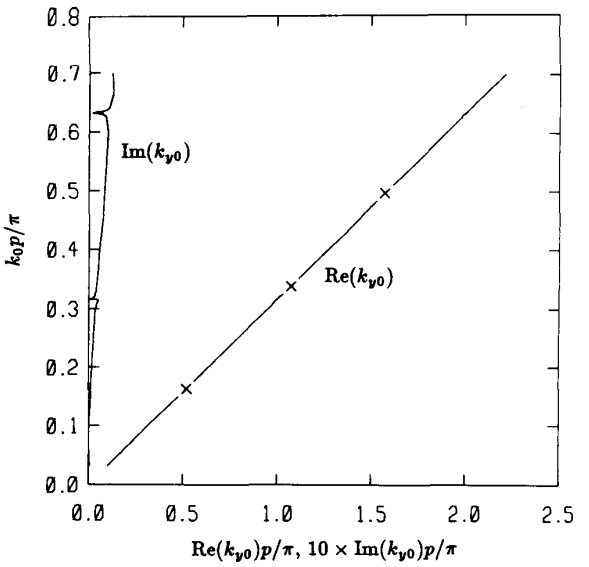

Fig. 12. The dispersion relation for one signal stripline periodically loaded with crossing strips of infinite length, $\epsilon_r = 10$, $t_1 = t_2 = t_3 = 0.2$ mm, $p = 2.5$ mm, $w_1 = w_c = 0.125$ mm, $h = \lambda_e/8$, $m = 6$, $\times$: $m = 14$.

flowing away from the signal stripline. This traveling wave surface current guides some power away from the signal line and hence reduces the guided power along the signal line.

In this case, the passband–stopband behavior which is characteristic of periodic structures does not appear. The wavenumber k_{y0} has a nonzero imaginary part over all frequencies. This is due to the power guided by the traveling wave along the crossing strips. Around $k_{y0} = n\pi/p$, the separation between two neighboring crossing strips is $n\lambda/2$, where λ is the wavelength of the guided mode. The power carried by the crossing strips at these frequencies is very small because the current on the signal line has opposite phase on the two sides of the crossing strip. Also, in this case, the higher order waveguide mode is not excited.

V. Conclusions

A rigorous dyadic Green's function formulation for the periodic structure is derived to study the dispersion properties of single and coupled signal lines periodically loaded with crossing strips. The passband and stopband characteristics are investigated when crossing strips are of finite or infinite length.

For crossing strips of finite length, the stopband properties are mainly affected by the period, the length of crossing strips, and the separation between the signal and crossing strips. Also, at higher frequencies, higher order stopbands occur. For crossing strips of infinite length, attenuation along the signal line exists over the whole frequency range due to the power guided by the traveling wave along crossing strips.

REFERENCES

[1] T. Kitazawa and R. Mittra, "An investigation of striplines and fin lines with periodic stubs," *IEEE Trans. Microwave Theory Tech.*, vol. MTT-32, pp. 684–688, July 1984.

[2] Y. Fukuoka and T. Itoh, "Slow-wave coplanar waveguide on periodically doped semiconductor substrate," *IEEE Trans. Microwave Theory Tech.*, vol. MTT-31, pp. 1013–1017, Dec. 1983.

[3] Q. Gu and J. A. Kong, "Transient analysis of single and coupled lines with capacitively loaded junctions," *IEEE Trans. Microwave Theory Tech.*, vol. MTT-34, pp. 952–964, Sept. 1986.

[4] B. J. Rubin, "The propagation characteristics of signal lines in a mesh-plane environment," *IEEE Trans. Microwave Theory Tech.*, vol. MTT-32, pp. 522–531, May 1984.

[5] C. H. Chan and R. Mittra, "The propagation characteristics of signal lines embedded in a multilayered structure in the presence of a periodically perforated ground plane," *IEEE Trans. Microwave Theory Tech.*, vol. MTT-36, pp. 968–975, June 1988.

[6] N. V. Nair and A. K. Mallick, "An analysis of a width-modulated microstrip periodic structure," *IEEE Trans. Microwave Theory Tech.*, vol. MTT-32, pp. 200–204, Feb. 1984.

[7] F. J. Glandorf and I. Wolff, "A spectral-domain analysis of periodically nonuniform microstrip lines," *IEEE Trans. Microwave Theory Tech.*, vol. MTT-35, pp. 336–343, Mar. 1987.

[8] J. A. Kong, *Electromagnetic Wave Theory*. New York: Wiley, 1986.

[9] R. W. Jackson and D. M. Pozar, "Full-wave analysis of microstrip open-end and gap discontinuities," *IEEE Trans. Microwave Theory Tech.*, vol. MTT-33, pp. 1036–1042, Oct. 1985.

[10] H. Y. Yang and N. G. Alexopoulos, "A dynamic model for microstrip-slotline transition and related structures," *IEEE Trans. Microwave Theory Tech.*, vol. 36, pp. 286–293, Feb. 1988.

[11] E. H. Newman and D. Forrai, "Scattering from a microstrip patch," *IEEE Trans. Antennas Propagat.*, vol. AP-35, pp. 245–251, Mar. 1987.

✠

Jean-Fu Kiang was born in Taipei, Taiwan, R.O.C., on February 2, 1957. He received the B.S. and M.S. degrees in electrical engineering from National Taiwan University in 1979 and 1981, respectively. In 1983, he became a research and teaching assistant in the Department of Electrical Engineering and Computer Science at the Massachusetts Institute of Technology, Cambridge, MA, where he is pursuing the Ph.D. degree. His research interests are electromagnetic theory, applications, and numerical analysis.

Mr. Kiang is a member of Sigma Xi.

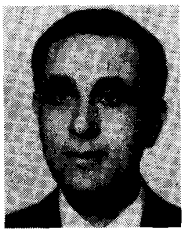

Sami M. Ali (M'79–SM'86) was born in Egypt on December 7, 1938. He received the B.S. degree from the Military Technical College, Cairo, Egypt, in 1965, and the Ph.D. degree from the Technical University of Prague, Prague, Czechoslovakia, in 1975, both in electrical engineering.

He joined the Electrical Engineering Department, Military Technical College, Cairo, in 1975. From 1981 to 1982 he was a visiting scientist at the Research Laboratory of Electronics, Massachusetts Institute of Technology, Cambridge, MA. In 1985, he became a Professor and head of the Basic Electrical Engineering Department, Military Technical College, Cairo, Egypt. Since 1987, he has been a visiting scientist at the Research Laboratory of Electronics at M.I.T. His current research interests deal with microwave integrated circuits and microstrip antenna applications.

✠

Jin Au Kong (S'65–M'69–SM'74–F'85) is Professor of Electrical Engineering and Chairman of Area IV on Energy and Electromagnetic Systems in the Department of Electrical Engineering and Computer Science at the Massachusetts Institute of Technology, Cambridge, MA. In 1977–80 he served the United Nations as a High-Level Consultant to the Under-Secretary-General on Science and Technology, and as an Interregional Advisor on remote sensing technology for the Department of Technical Cooperation for Development. His research interest is in the area of electromagnetic wave theory and applications.

Dr. Kong has published five books, 123 refereed journal articles, and 125 conference papers, and has supervised 77 theses. He is currently a member of the Advisory Council for the Electrical Engineering Department at the University of Pennsylvania, a consultant to the M.I.T. Lincoln Laboratory, the Editor for the Wiley series on remote sensing, the Editor-in-Chief of the *Journal of Electromagnetic Waves and Applications* (JEWA), and the Chief Editor for the Elsevier book series on Progress In Electromagnetics Research (PIER).